Transactions on Ecology and the Environment vol 2, © 1993 WIT Press, www.witpress.com, ISSN 1743-3541

Global climate change effects on water quality in aquatic ecosystems

C. Jokiel,[a] G. Meyer,[b] G.T. Orlob,[b] G. Rouvé[a]
[a] *Institute for Hydraulic Engineering and Water Resources Management (IWW), Aachen, University of Technology (RWTH), W-5100 Aachen, Germany*
[b] *Department of Civil and Environmental Engineering, University of California, Davis 95616, USA*

ABSTRACT

The prospect of gradual change in the earth's climate regime due to anthropogenic influences has resulted in considerable speculation, e.g. changes in the frequency and severity of droughts, floods, or other climate related disturbances. Within this paper the impacts of climate changes on the quality of natural and artificial water bodies due to atmosphere-hydrosphere interactions are described. We used a heat energie balance approach to determine the changes in the water temperature and related changes in the dissolved oxygen concentration due to an increase in mean atmospheric temperature in the Shasta-Trinity-System and the Sacramento River located in the Central Valley of California.

INTRODUCTION

Aquatic ecosystems are highly influenced by numerous exchange processes, e.g. precipitation, evaporation, radiation, between atmosphere and hydrosphere. Therefore, changes of any of the principal atmospheric variables (temperature, vapor pressure, humidity, air quality) and the hydrologic cycle evoke significant impacts on the reservoirs of water mass (solid, liquid, gas), their thermal energy and related water quality. For example, a change in air temperature elevates the snow line in mountainous regions, increases the melt rate, and thus shifts the quantity and timing of the flux of cold water. On the other hand, surface water temperatures will increase due to temperature exchanges with the warmer atmosphere.

The extreme complex physical, chemical and biological interactions between atmospheric, hydrologic and water quality variables do not yet allow the simulation of all these processes. However, there are useful approaches which can represent the essential key interactions between the atmosphere and hydrosphere. Application of such models will be explained in the following section.

HEAT ENERGY BALANCE

The net change of thermal energy in a control volume in a surface water body is the sum of net heat exchange at the air-water interface q_n, the flux of heat to and from the bottom sediments q_c and the amount of external heat entering or leaving the control volume q_t. The source and sink term for the full heat balance to predict the one-dimensional distribution of thermal energy can be written as

$$\frac{\partial \theta}{\partial t} = (q_n + q_c + q_t) \cdot \frac{1}{c_p \cdot \rho \cdot h} \qquad (1)$$

where:

θ	water temperature [°C]
t	time [min]
q_n	net heat exchange at air-water interface [ly/min]
q_c	net heat exchange at ground-water interface [ly/min]
q_t	external heat inflows and outflows [ly/min]
c_p	specific heat capacity [cal/g/°C]
ρ	density [g/cm^3]
h	depth of flow [cm]

The effects of climate changes on the heat balance are incorporated into the components of q_n and q_c.

<u>Net heat exchange at the air-water interface, q_n</u>

Figure 1 shows the five components describing the net heat exchange at the air-water interface with typical values.

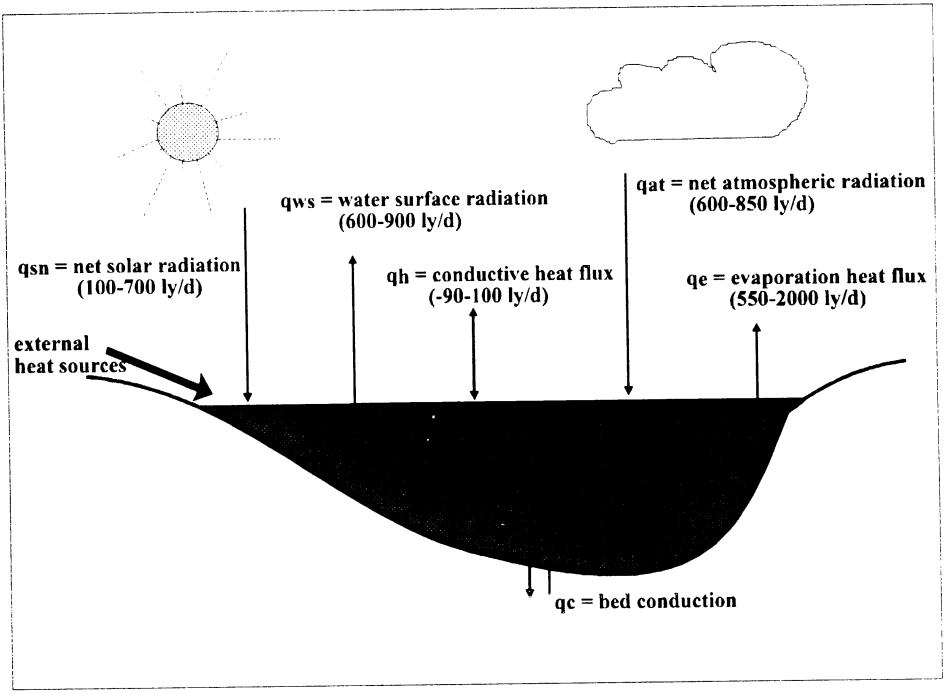

Fig. 1: Components of net heat exchange with typical values

Each of these components is affected by the properties of the atmosphere, some depend on the water temperature, and some are interrelated.

$$q_n = q_{sn} + q_{at} + q_{ws} + q_e + q_h \qquad (2)$$

Within equation 2 the main heat sources are the net short wave radiation q_{sn} which can be described as the solar beam radiation reduced by scattering and absorption in the atmosphere and the long wave radiation q_{at} from the overlying air mass. Long wave radiation is mainly influenced by air temperature and humidity. Evaporation q_e driven by the vapor gradient between the water surface and the dry air above and long wave back radiation from the waterbody q_{ws} based on the Stefan-Boltzman law cause heat losses into the atmosphere. The most common approach to compute the sensible heat flux q_h is to relate it to the evaporation flux by means of the Bowen ratio. It is a function of the temperature differences between water and air.

The equations for the different components are given below. For detailed information of their derivations and alternative approaches we refer to Meyer and Orlob [1] and McCutcheon [2].

-Net solar short wave radiation q_{sn}

$$q_{sn} = q_0 \cdot a_t \cdot \left(1 - 0.65C^2\right) \cdot \left(1 - R_s\right) \quad (3)$$

where:

q_0 radiation intensity at the top of the earth's atmosphere [ly/min]
a_t atmospheric transmission term
C cloudiness as fraction of sky covered [%]
R_s water surface reflectivity = 0.03

-Net atmospheric long wave radiation q_{at}

$$q_{at} = 0.937 \cdot 10^{-6} \cdot \sigma \cdot T_a^6 \cdot \left(1 + 0.17C^2\right) \cdot \left(1 - R_s\right) \quad (4)$$

where:

σ Stefan-Bolzman constant = $8.125 \cdot 10^{-11}$ [ly/min]
T_a absolute air temperature [°K]

-Water surface radiation q_{ws}

$$q_{ws} = \varepsilon \cdot \sigma \cdot T_{ws}^6 \quad (5)$$

where:

T_{ws} temperature of water surface [°K]
ε emissivity for a water surface = 0.97

-Evaporation heat flux q_e

$$q_e = \rho_w \cdot L_v \cdot E \quad (6)$$

where:

ρ_w water density [g/cm^3]

L latent heat of vaporazation = $597.1-0.57 \cdot \theta_0$ [cal/g]

θ_0 average water surface temperature [°C]
E net evaporation rate [cm/min]

-Sensible (conductive) heat flux q_e

$$q_h = q_e \cdot B \quad (7)$$

where:

B Bowen's ratio = $0.66 \cdot \left[\dfrac{\theta_o - \theta_a}{e_o - e_a}\right] \cdot \dfrac{p}{p_o}$

θ_0 water surface temperature [°C]

θ_a dry bulb air temperature [°C]
e_0 saturation vapor pressure at water surface temperature [mbar]
e_a actual vapor pressure [mbar]

P_0 atmospheric pressure [mbar]
P atmospheric pressure at sea level = 1013 [mbar]

Substituting equations 3-7 into equation 2 leads to a complex function for the net heat exchange q_n which allows estimation of the value of q_n for a given water temperature θ_0.

Net heat exchange at the ground-water interface q_c

The bed conduction is proportional to the gradient of temperature in the soil-water medium. Thus the ground-water heat flux becomes

$$q_c = K_g \cdot \frac{(\theta_0 - \theta_g)}{z} \tag{8}$$

where:
K_g conductivity coefficient [ly·m/min/°C]
θ_0 water surface temperature [°C]
θ_g soil-water temperature [°C] at depth z [m]

Bed conduction is important when predicting the diel evolution of temperature in a shallow stream.

Equilibrium Temperature

The equilibrium temperature θ_e is that temperature at which the net heat flux becomes zero.

$$q_{nc} = q_n(\theta) + q_c(\theta) = 0 \tag{9}$$

With given specific atmospheric conditions the exogenous fluxes q_{sn} and q_{at} are known and the water temperature balancing the components q_{ws}, q_e, q_h and q_c, of equation 9 can be determined. This temperature is the so-called "equilibrium temperature", θ_e.

The rate of change of temperature within the water body is given by

$$c_p \cdot \rho \cdot h \frac{\partial \theta}{\partial t} = \frac{\partial q_n}{\partial t}(\theta - \theta_e) = K(\theta - \theta_e) \tag{10}$$

Integration of equation 10 with respect to time leads to

$$\theta_t = \theta_e + (\theta_1 - \theta_e) \cdot \exp\left[\frac{-k \cdot t}{c_p \cdot \rho \cdot h}\right] \tag{11}$$

which states that under steady state conditions the water temperature tends towards the equilibrium temperature.

CASE STUDY: CENTRAL VALLEY CALIFORNIA

The heat energy balance approach for predicting water temperature changes due to atmospheric changes is applied to a river-reservoir-system in the Central Valley of California (fig. 2).

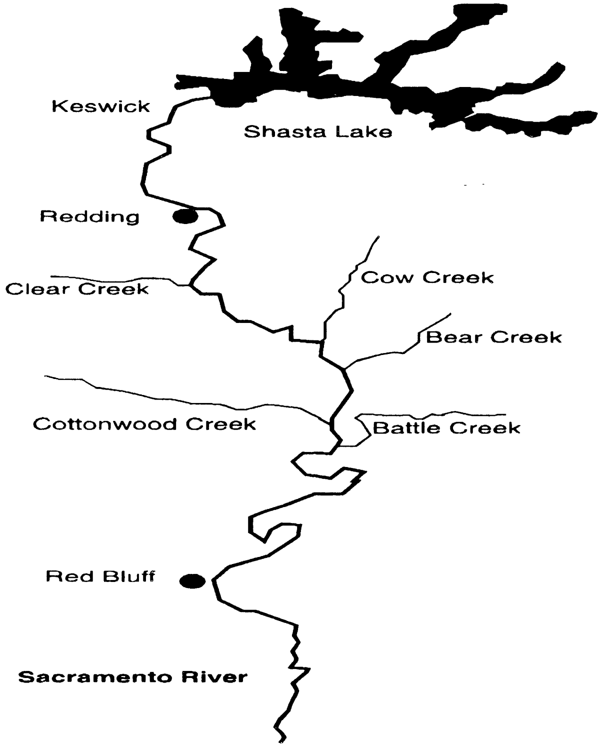

Figure 2: Shasta-Reservoir and Sacramento-River System

Releases from the Shasta-Trinity-Reservoir-System discharge into the Sacramento River, the habitant for salmon species. To guarantee an undisturbed evolution of this species fresh water with temperatures below 13°C are required. Otherwise the normal cycle of development will be interrupted.

Field investigations and modeling studies of stream and reservoir temperatures have demonstrated that the Sacramento River spawning areas are controlled by discharges of cold water from upstream impoundments. Climate changes, e.g. due to a doubling of CO_2, could endanger the habitant for salmon.

This case study outlines the consequences of climate changes on the water quality within the Shasta Reservoir and the Sacramento River emphasizing temperature.

Climate change scenarios and boundary conditions

Two scenarios, simulating temperature and dissolved oxygen in the Shasta Lake and the Sacramento River, will be compared. Scenario I is the base case which has been developed using historic meteorological, water quality and reservoir operation data. According to hydrologic and meteorologic predictions by Global Climate Models (GCM's) scenario II (doubling of CO_2) is generated. The key boundary conditions of the base case and the $2xCO_2$ scenario are summarized in figure 3.

	Base Case, 1x CO2					Climate Change, 2 x CO2				
Month	Air Temp. °C	Dew P. Temp. °C	Wind m/s	Sky Cover fraction	Runoff m³/s	Air Temp. °C	Dew P. Temp. °C	Wind m/s	Sky Cover fraction	Runoff m³/s
Jan	8.06	0.13	2.86	0.66	250.00	11.89	4.92	4.01	0.77	310.00
Feb	10.67	1.21	3.22	0.55	360.00	14.58	5.85	5.69	0.73	560.00
Mar	12.44	3.51	3.62	0.60	460.00	16.59	7.63	5.1	0.84	900.00
Apr	15.67	5.36	3.40	0.62	250.00	20.16	8.68	2.56	0.53	250.00
May	20.39	6.62	3.75	0.49	200.00	25.23	9.13	2.7	0.25	200.00
Jun	24.94	8.93	3.67	0.37	120.00	30.05	10.78	4.19	0.29	120.00
Jul	28.61	9.78	3.31	0.16	110.00	33.82	11.34	3.12	0.1	110.00
Aug	27.33	9.21	3.04	0.20	100.00	32.46	10.92	2.13	0.13	100.00
Sep	24.56	6.84	2.99	0.26	110.00	29.43	9.11	1.4	0.12	110.00
Oct	19.00	6.32	2.91	0.36	120.00	23.54	9.38	3.9	0.51	120.00
Nov	12.11	4.63	2.91	0.53	140.00	16.3	8.53	2.37	0.66	120.00
Dec	8.50	1.26	3.08	0.54	250.00	12.43	5.77	2.8	0.37	125.00

Fig. 3: Key boundary conditions: Base case and $2xCO_2$ Scenarios

Tributary inflow temperatures were calculated with the equilibrium temperature approach. Following the method outlined in section 2 the equilibrium temperature was calculated for each month of the year, using historic mean values of the key parameters as noted above. Comparison of the calculated equilibrium temperatures for the head waters with those observed under historic conditions, as shown in figure 4, reveals a good approximation of the annual temperature cycle. The same procedure was applied for the $2xCO_2$ scenario to evaluate the changed inflow temperatures.

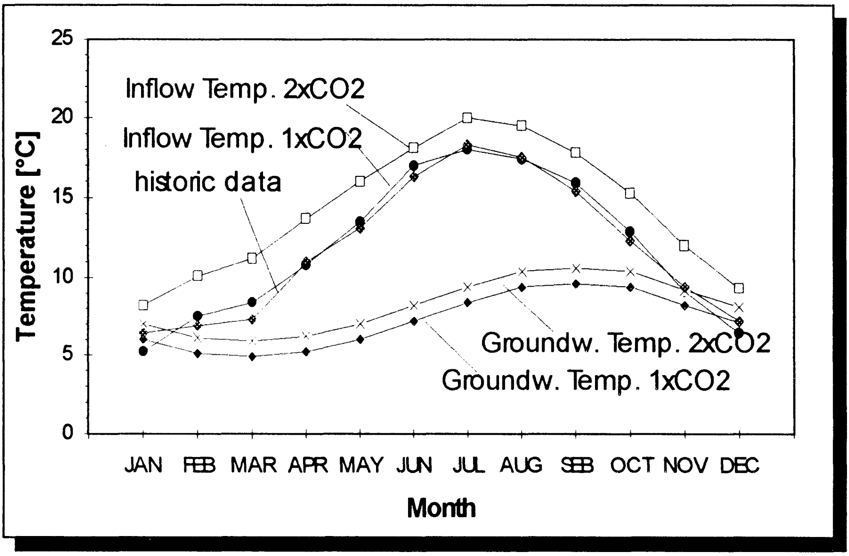

Fig. 4: Historic inflow temperatures and calculated inflow temperatures

Simulation results, Shasta Lake

Figure 5 shows the outflow temperatures through the penstock of Shasta powerhouse for the two cases, which in turn define the headwater conditions for the Sacramento River. The outlet temperatures for the $2xCO_2$ scenario are about 2 to 4°C higher than in the base case. Note that the period during which the outlet temperature exceeds the threshold increases also.

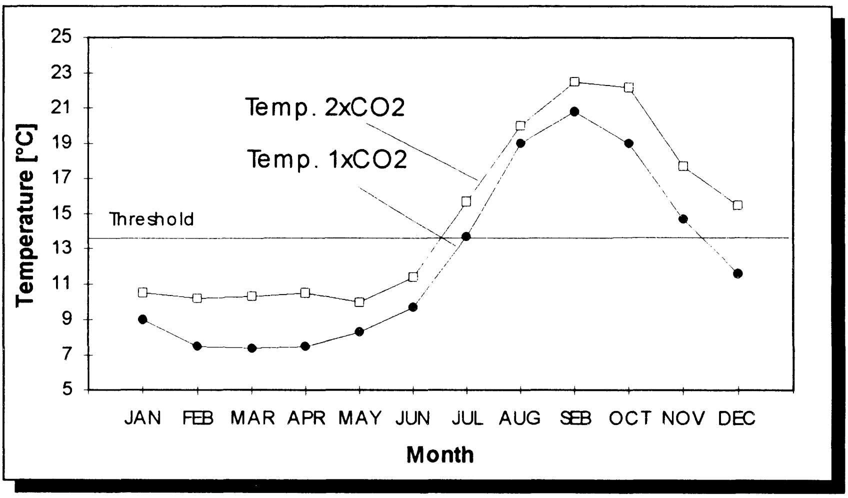

Fig. 5: Outflow temperatures through Shasta Powerhouse

Transactions on Ecology and the Environment vol 2, © 1993 WIT Press, www.witpress.com, ISSN 1743-3541

Simulation results Sacramento River

Meteorological boundary conditions for the Sacramento River are taken equal to those of Shasta Lake (fig. 3). Headwater flows are provided by releases from Shasta Lake. Dissolved oxygen concentrations taken as input to the Sacramento River are slightly below saturation in the tributaries.

Figure 6 illustrates the yearly distribution of temperature and dissolved oxygen at Red Bluff, at the downstream end of the simulated river reach, approximately the limit of salmon spawning area. The cycle is typical for a river in the middle latitudes of the nothern hemisphere, with the lowest levels in January and February and peak levels in August and September.

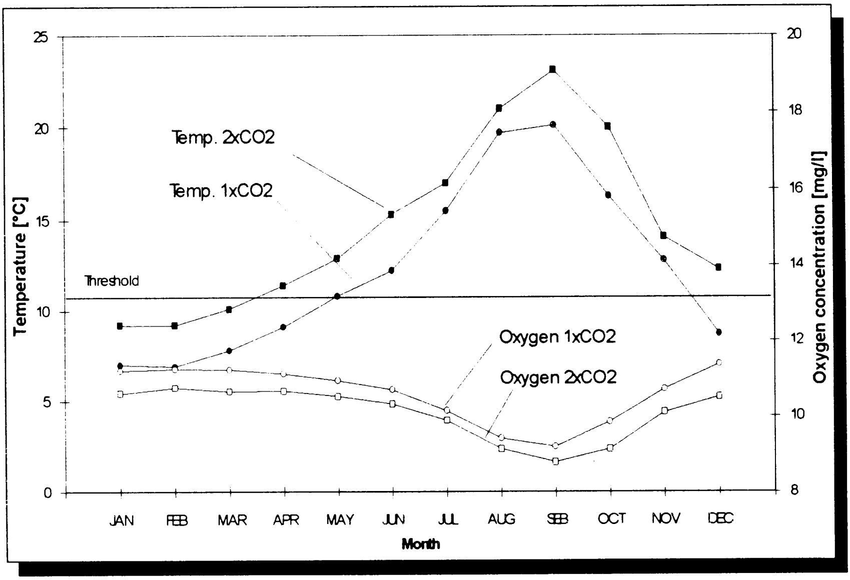

Fig. 6: Yearly distribution of temperatures and oxygen concentrations at Red Bluff

In the 2xCO_2 scenario temperatures are higher throughout the whole year with differences between 1.5 and 4 °C. The period when temperatures are above 13.3 °C is prolonged to about seven months seriously endangering the salmon habitant.

The distribution of dissolved oxygen over the year is governed mainly by the effect of temperature on oxygen saturation. For example an increase in temperature due to climate change is accompanied by a decrease in dissolved oxygen concentration.

CONCLUSIONS

A heat energy balance approach has been presented and used to determine the impacts of climate change, due to a doubling of CO_2 in the atmosphere, on water quality. The primary impacts are changes in temperature and hydrologic fluxes to Shasta Lake and the Sacramento River. The effects on the temperature and dissolved oxygen concentrations in the river downstream induced by these changed boundary conditions are illustrated. The temperature, already endangering the spawning fish, would be further increased and the period of critical conditions further extended. Dissolved oxygen concentrations decrease significantly, primarily due to the associated increase in water temperature.

Further secondary impacts of climate changes on the aquatic environment, e.g. increases of nutrients and organics, or variation in biological cycles, are subjects for future investigations.

References

1. Orlob, G.T.; Meyer G.K.: "Impacts of Climate Change on Water Quality and Aquatic Ecosystems", Chapter 5,(In Press), 1992

2. Orlob, G.T.; Meyer, G.K. Jokiel, C.: "Climate Change Effects on Water Quality: Central Valley California", Chapter13,(In Press), 1992

3. McCutcheon, S. C.: "Water Quality Modeling", CRC Press, Inc., Boca Raton, Florida, 1989

4. Schroeder, E. ; Tchobanoglous, G.: "Water Quality", Addison-Wesley Publishing Company Inc., New York, 1987